Fermion-induced effective action in the presence of a static inhomogeneous magnetic field

Pavlos Pasipoularides*
Department of Physics, National Technical University of Athens, Zografou Campus, 157 80 Athens, Greece
(Received 18 December 2000; revised manuscript received 6 June 2001; published 19 October 2001)

We present a numerical study of the fermion-induced effective action in the presence of a static inhomogeneous magnetic field for both $(3+1)$- and $(2+1)$-dimensional QED using a novel approach. This approach is appropriate for cylindrically symmetric magnetic fields with a finite magnetic flux Φ. We consider families of magnetic fields, dependent on two parameters: a typical value B_m for the field and a typical range d. We investigate the behavior of the effective action for three distinct cases: (1) keeping Φ (or $B_m d^2$) constant and varying d, (2) keeping B_m constant and varying d, and (3) keeping d constant and varying Φ (or $B_m d^2$). We note an interesting difference in the limit $d \to +\infty$ (case 2) between smooth and discontinuous magnetic fields. In the strong field limit (case 3) we also derive an explicit asymptotic formula for the $(3+1)$-dimensional action. We study the stability of the magnetic field and show that magnetic fields of the type we examine remain unstable, even in the presence of fermions. In the appropriate regions we check our numerical results against the Schwinger formula (constant magnetic field), the derivative expansion, and the numerical work of Bordag and Kirsten. The role of the Landau levels in the effective action and the appearance of metastable states for a large magnetic flux are discussed in the Appendixes.

DOI: 10.1103/PhysRevD.64.105011 PACS number(s): 11.15.Tk

I. INTRODUCTION

The evaluation of the fermion-induced effective action in the presence of a static magnetic field is important in quantum electrodynamics. Historically, the effective action for a homogeneous magnetic field was first computed by Heisenberg and Euler [1], then by Weisskopf [2], and later by Schwinger [3] with the proper time method. The effective action in this case can be expressed by an explicit formula. In Ref. [4] Redlich obtained the corresponding results for $(2+1)$-dimensional QED.

For inhomogeneous magnetic fields explicit formulas are not available. Approximations can be developed for the case of (a) weak magnetic fields (perturbative expansion) and (b) smooth magnetic fields (derivative expansion). More recently, for a special form of the magnetic field it has been possible to derive a closed formula for the effective action for both $3+1$ and $2+1$ dimensions [5,6]. Another exact result is presented in Ref. [7], for a magnetic field with a delta function profile in two-dimensional Euclidean space.

The aim of this paper is to obtain, by *numerical* computations, qualitative knowledge of the dependence of the fermion-induced effective action on various quantities characterizing the magnetic field such as its size and its degree of inhomogenity, etc. For this numerical study we use a simple novel approach for the fast computation of the effective action, which is appropriate for static, cylindrically symmetric magnetic fields with a finite magnetic flux Φ. We will call such fields magnetic flux tubes.

Previous numerical studies of the effective action are the following. In Ref. [8] the effective energy, in $3+1$ dimensions, was computed numerically for a cylindrically symmetric static magnetic field which is constant inside a cylinder and zero outside it. In more recent work [9] the effective action was computed for a cylindrically symmetric static magnetic field with a delta function profile, in $3+1$ dimensions. Note that this field has infinite classical energy.

Our purpose in this paper is to go beyond the previous numerical work, and to study, for the first time, the $2+1$ QED effective energy in the presence of a magnetic flux tube. In addition, in the case of $3+1$ dimensions we consider more realistic magnetic field configurations than those of the previous work, for example, the Gaussian magnetic field of Eq. (2) below.

We study families of magnetic fields dependent on two parameters, a typical value[1] B_m for the field (or the magnetic flux $\Phi = B_m d^2/2$) and a typical range d. We investigate the behavior of the effective action for three distinct cases: (1) keeping Φ (or $B_m d^2$) constant and varying d, (2) keeping B_m constant and varying d, and (3) keeping d constant and varying Φ (or $B_m d^2$). The mass of the fermion m_f is assumed to be constant.

We note a difference in the limit $d \to +\infty$ (case 2) between smooth and discontinuous magnetic fields (Sec. V). We will see that this difference is related to the fact that the derivative expansion fails for discontinuous magnetic fields like the magnetic field of Eq. (3) below.

An interesting problem not covered by previous work is the behavior of the effective energy for large magnetic flux ϕ (strong magnetic field) and fixed $m_f d$, where $\phi = e\Phi/2\pi$. In Sec. VII we present an investigation for large ϕ. In particular, in the case of $3+1$ dimensions, we derive an explicit asymptotic formula for $\phi \gg 1$.

We also consider the question of stability of the magnetic field in the presence of fermions. The question is whether some radius exists that minimizes the total energy (classical

*Electronic address: paul@central.ntua.gr

[1]We define this typical magnetic field strength as $B_m = \int \vec{B} \cdot d\vec{S}/\pi d^2$.

energy plus effective energy) for fixed magnetic flux Φ, thus rendering the magnetic field stable at the quantum level. The same question was considered by the authors of Ref. [8], for the magnetic field of Eq. (3) (below) in the case of $3+1$ dimensions, and the answer was negative. Our purpose here is to study the stability of magnetic flux tubes in the case of $2+1$ dimensions. In addition, in the case of $3+1$ dimensions, we generalize the results of Ref. [8] for more realistic magnetic field configurations like the Gaussian magnetic field of Eq. (3). Note that we answer this question for several two-parameter families of magnetic field configurations of the type of the flux tube for both $2+1$ and $3+1$ dimensions (see the magnetic fields at the end of the present section).

In Appendix C we explain the role of the Landau levels in the effective action, relating them to the metastable states that appear in the case of large magnetic flux Φ (see Appendix B).

The vector potential and the magnetic field for the class of magnetic fields we examine are given by the following equations:

$$\vec{A}(r)=\frac{r}{2}f(r)\vec{e}_{\phi},\quad \vec{B}(r)=\frac{1}{2r}\frac{d}{dr}[r^2 f(r)]\vec{e}_z, \tag{1}$$

where $f(r)$ is a function with asymptotic behavior $2\phi/r^2$ as r tends to infinity and $\phi=e\Phi/2\pi$. In what follows, we assume the rescaling $B\to eB$ except where we state otherwise. We present our numerical results for two magnetic fields, one with a Gaussian profile and one that is constant inside and vanishes abruptly outside a cylinder of radius d, with respective field strengths

$$B_1(r)=\frac{2\phi}{d^2}\exp\left(-\frac{r^2}{d^2}\right), \tag{2}$$

$$B_2(r)=\frac{2\phi}{d^2}\theta(d-r), \tag{3}$$

where $\theta(x)$ is the step function.

We have performed analogous calculations for six two-parameter families of magnetic fields other than those of Eqs. (2) and (3), with magnetic field strengths

$$B_3(r)=\frac{2\phi}{d^2}\frac{1}{\cosh^2(r^2/d^2)},$$

$$B_4(r)=\frac{4\phi}{d^2}\left(\frac{r^2}{d^2}\right)\exp\left(-\frac{r^4}{d^4}\right),$$

$$B_5(r)=\frac{4\phi}{d^2\pi}\frac{1}{(r^4/d^4+1)},$$

$$B_6(r)=\frac{6\phi}{d^2}\left(1-\frac{r}{d}\right)\theta(d-r),$$

$$B_7(r)=\frac{4\phi}{d^2}\left(1-\frac{r^2}{d^2}\right)\theta(d-r),$$

$$B_8(r)=\frac{2\phi}{d^2}\frac{1}{(r^2/d^2+1)^2}.$$

Since including the results in detail would make this paper unnecessarily long it is perhaps sufficient to state that our conclusions (about the stability of the magnetic field or the dependence on d of the effective action, etc.) for the magnetic fields of Eqs. (2) and (3) are valid also for the above-mentioned magnetic fields.

II. EFFECTIVE ENERGY

We consider the following path integral that corresponds to QED:

$$Z=\int \mathcal{D}A\mathcal{D}\bar{\Psi}\mathcal{D}\Psi\exp\left(i\int d^Dx\left[-\frac{1}{4}F_{\mu\nu}F^{\mu\nu}+\bar{\Psi}(i\not{D}-m_f)\Psi\right]\right) \tag{4}$$

in dimension D ($D=3,4$). Integrating out the fermionic degrees of freedom in the above-mentioned path integral, we obtain the effective action expressed as the logarithm of a determinant:

$$S_{eff}[A]=\frac{1}{i}\ln\int \mathcal{D}\bar{\Psi}\mathcal{D}\Psi\exp\left(i\int d^Dx\bar{\Psi}(i\not{D}-m_f)\Psi\right)=\frac{1}{i}\mathrm{tr}\ln(i\not{D}-m_f) \tag{5}$$

where $\not{D}=\gamma^\mu(\partial_\mu-ieA_\mu)$, and $\gamma^0=\sigma_3$, $\gamma^1=i\sigma_1$, $\gamma^2=i\sigma_2$ is a two-component representation of the gamma matrices for the $(2+1)$-dimensional QED. A four-component representation will be used for the $(3+1)$-dimensional case.

We will use the identity

$$\mathrm{tr}\ln(i\not{D}-m_f)=\frac{1}{2}\mathrm{tr}\ln(\not{D}^2+m_f^2) \tag{6}$$

in order to take advantage of the diagonal form of the operator $\not{D}^2+m_f^2$. It is well known that for $(2+1)$-dimensional QED a parity violating term (Chern-Simons term) is induced [4,10]. However, this term is zero for the case we investigate.[2] See also the relevant comments in Ref. [11].

We deal first with the $(2+1)$-dimensional problem. The operator $\not{D}^2+m_f^2$ for a static magnetic field can be put into the form

[2]The induced Chern-Simons term is of the form $(\kappa/2)\int d^3x\varepsilon^{\mu\nu\rho}A_\mu\partial_\nu A_\rho$ and it is zero for our case, since $A_0=0$ and $\dot{A}_1=\dot{A}_2=0$.

$$\not{D}^2+m_f^2=\partial_0^2+(\gamma^m D_m)^2+m_f^2 \quad (m=1,2). \tag{7}$$

This operator has a complete system of eigenfunctions of the form $\Psi_{\{n\}}(\vec{x},t)=e^{-i\omega t}\Psi_{\{n\}}(\vec{x})$ where $\Psi_{\{n\}}(\vec{x})$ satisfies the eigenvalue equation $(\gamma^m D_m)^2\Psi_{\{n\}}(\vec{x})=E_{\{n\}}\Psi_{\{n\}}(\vec{x})$ and $\{n\}$ is a set of quantum numbers. Note that $E_{\{n\}}\geqslant 0$ since the operator $(\gamma^m D_m)^2$ is positive definite as the square of a Hermitian operator. It is convenient here to refer to the effective energy $E_{eff}=-S_{eff}/T$ instead of the effective action S_{eff}, where T is the total length of time. The effective energy, if we perform a Wick rotation of the integration variable ω $(\omega\rightarrow i\omega)$, is given by

$$E_{eff(2+1)}=-\frac{1}{2\pi}\sum_{\{n\}}\int_0^{+\infty}d\omega\,\ln(\omega^2+E_{\{n\}}+m_f^2). \tag{8}$$

We make the above integral convergent by subtracting a term that is independent of the magnetic field. We may do so because our purpose is to compute the difference between the effective energy in the presence of the magnetic field, and the energy when the magnetic field is absent. If we subtract the term $-(1/2\pi)\Sigma_{\{n\}}\int_0^{+\infty}d\omega\,\ln(\omega^2+m_f^2)$ from Eq. (8) and integrate, we get

$$E_{eff(2+1)}=-\frac{1}{2}\sum_{\{n\}}(\sqrt{E_{\{n\}}+m_f^2}-m_f). \tag{9}$$

This expression incorporates the expectation that very massive fermions interact weakly with the magnetic flux tube (i.e., the effective energy tends to zero as m_f tends to infinity).

The extension to the $(3+1)$-dimensional case can be made if we replace m_f^2 by $k_3^2+m_f^2$ in Eq. (9) and integrate over the k_3 momentum. An overall factor of 2 (from the Dirac trace) must also be included (for details see, e.g., Ref. [6]):

$$E_{eff(3+1)}=-L_z\sum_{\{n\}}\int_{-\infty}^{+\infty}\frac{dk_3}{2\pi}(\sqrt{k_3^2+E_{\{n\}}+m_f^2}-\sqrt{k_3^2+m_f^2}) \tag{10}$$

where L_z is the length of the space box in the z direction.

Introducing a momentum cutoff $\Lambda/2$ we find

$$E_{eff(3+1)}=\frac{1}{4\pi}\sum_{\{n\}}(E_{\{n\}}+m_f^2)\ln\left(\frac{E_{\{n\}}+m_f^2}{m_f^2}\right)-\frac{1}{4\pi}\sum_{\{n\}}E_{\{n\}}-\frac{1}{4\pi}\ln\left(\frac{\Lambda^2}{m_f^2}\right)\sum_{\{n\}}E_{\{n\}} \tag{11}$$

where we have omitted L_z and we assume that we calculate energy per unit length.

For large m_f the above expression for the effective energy must tend to the first diagram (vacuum polarization diagram) of the perturbative expansion of the effective energy:

$$E^{(2)}_{eff(3+1)}=-\frac{1}{8\pi^3}\int_0^1 dx\,x(1-x)\times\int_0^{+\infty}dq\,q|\tilde{B}(q)|^2\ln\left(\frac{m_f^2+q^2x(1-x)}{m_f^2}\right)+\frac{1}{24\pi^2}\ln\left(\frac{\Lambda^2}{m_f^2}\right)\int d^2\vec{x}B^2(\vec{x}) \tag{12}$$

where $\tilde{B}(q)=\int d^2\vec{x}e^{-i\vec{q}\cdot\vec{x}}B(\vec{x})$. Note that $\tilde{B}(q)$ depends only on $q=|\vec{q}|$ as we have assumed that the magnetic field is cylindrically symmetric.

If we compare Eqs. (11) and (12) for $m_f\rightarrow\infty$ we find

$$\sum_{\{n\}}E_{\{n\}}=-\frac{1}{6\pi}\int d^2\vec{x}B^2(\vec{x}). \tag{13}$$

Thus, the logarithmically divergent part in Eq. (11) can be dropped if we include an appropriate counterterm in the QED Lagrangian. This counterterm is defined by the on-shell renormalization condition[3] $\Pi(0)=0$. The renormalized effective energy is then given by the equation

$$E^{(ren)}_{eff(3+1)}=\frac{1}{4\pi}\sum_{\{n\}}(E_{\{n\}}+m_f^2)\ln\left(\frac{E_{\{n\}}+m_f^2}{m_f^2}\right)-\frac{1}{4\pi}\sum_{\{n\}}E_{\{n\}}. \tag{14}$$

Note that the renormalized effective energy vanishes for large values of m_f, as expected. For the sake of simplicity we will drop the index (ren) in the rest of this paper.

In order to define the effective action for massless fermions for which the right-hand side of Eq. (14) is singular, we should impose the renormalization condition for the vacuum polarization funtion $\Pi(q^2)$ at a spacelike momentum $-M^2$ $[\Pi(-M^2)=0]$. Accordingly, a formula for the effective action for massless fermions is given in Appendix A.

In cylindrical coordinates and for the special magnetic field of Eq. (1), the operator $(\gamma^m D_m)^2$ has the following diagonal form:

$$(\gamma^m D_m)^2=-D_1^2-D_2^2-sB=-\frac{\partial^2}{\partial r^2}-\frac{1}{r}\frac{\partial}{\partial r}-\frac{1}{r^2}\frac{\partial^2}{\partial\phi^2}-\frac{1}{i}\frac{\partial}{\partial\phi}f(r)+\frac{r^2f^2(r)}{4}-sB(r), \tag{15}$$

where s takes the values ± 1 which correspond to the two possible spin states of the electron. Because the operator

[3]For the definition of the vacuum polarization function $\Pi(q^2)$ and for details about the renormalization condition for $\Pi(q^2)$ see, for example, Ref. [12].

$(\gamma^m D_m)^2$ is invariant under rotations around the z axis, the eigenfunctions $\Psi_{\{n\}}(\vec{x})$ have the form $\Psi_{\{n\}}(\vec{x}) = e^{il\phi}u(r)/\sqrt{r}$, where l is the quantum number of the angular momentum ($l=0,\pm 1,\pm 2,\ldots$). The function $u(r)$ satisfies the equation

$$\left(-\frac{d^2}{dr^2}+\frac{l^2-\frac{1}{4}}{r^2}+v_{l,s}(r)\right)u(r)=k^2u(r) \tag{16}$$

where

$$v_{l,s}(r)=-lf(r)-sB(r)+\frac{r^2f^2(r)}{4} \tag{17}$$

and k^2 is the corresponding eigenvalue (we may set $E_{\{n\}}=k^2$ since $E_{\{n\}}\geqslant 0$). The spectrum of the radial Schrödinger equation (16), in addition to the continuous spectrum $(0,+\infty)$, may also have zero modes according to the Aharonov-Casher theorem[4] [13]. Note that for our special case $\{n\}=\{k,l,s\}$.

III. DENSITY OF STATES

In order to sum up over the continuous modes of Eq. (16), we shall need the density of states $dn/dk=\rho_{l,s}(k)$ (i.e., the number of states per unit k):

$$\rho_{l,s}(k)=\rho_{l,s}^{(free)}(k)+\frac{1}{\pi}\frac{d\delta_{l,s}(k)}{dk} \tag{18}$$

where $\rho_{l,s}^{(free)}(k)=\pi/L$ is the density of states for free space, and $\delta_{l,s}(k)$ is the phase shift that corresponds to the lth partial wave with momentum k and spin s. The relation (18) is shown, e.g., in Ref. [14].

A noteworthy feature of the function $\delta_{l,\sigma}(k)$ is that it exhibits jumps that correspond to metastable states for large values of ϕ. This is shown in Fig. 8 of Appendix A.

If we use the relations (18) and (9), the effective energy for $(2+1)$-dimensional QED is

$$E_{eff(2+1)}=-\frac{1}{2\pi}\int_0^{+\infty}(\sqrt{k^2+m_f^2}-m_f)\frac{d}{dk}\left[\sum_{l,s}\delta_{l,s}(k)\right]dk \tag{19}$$

where $\rho_{l,s}^{(free)}(k)$ was dropped since it contributes a field independent term. Note that the zero modes do not contribute explicitly in Eq. (19).

The series of the phase shifts over l in Eq. (19) is not absolutely convergent. The simplest way to define it is to sum symmetrically over l. We define the function

$$\Delta(k)=\lim_{L\to+\infty}\sum_{s,l=-L}^{L}\delta_{l,s}(k). \tag{20}$$

[4]According to this theorem a zero mode exists if the conditions $1<l+1<\phi$ and $s=1$ are satisfied.

The asymptotic behavior of the phase shifts for $|l|\gg kd$ is

$$\delta_{l,s}(k)\to\left(-\frac{|l-\phi|}{2}+\frac{|l|}{2}\right)\pi \tag{21}$$

and the sum $\delta_{l,s}(k)+\delta_{-l,s}(k)$ vanishes for large enough values of l so the limit in Eq. (20) exists.

The large l asymptotic behavior can be obtained from the WKB approximation for the phase shifts:

$$\delta_{l,s}(k)=\mathrm{Re}\left\{\int_0^{+\infty}\left(\sqrt{k^2-v_{l,s}(r)-\frac{l^2}{r^2}}-\sqrt{k^2-\frac{l^2}{r^2}}\right)dr\right\}. \tag{22}$$

For large l only the asymptotic $O(1/r^2)$ tail of the potential contributes to the above integral. Replacing $v_{l,s}(r)$ by its asymptotic form $(\phi^2-2\phi l)/r^2$ yields Eq. (21).

Note that an asymmetric sum would give the same result since $\lim_{L\to+\infty}\Sigma_{s,l=-L}^{L+\Delta L}\delta_{l,s}(k)=\Delta(k)+c'$ and c' is independent of k.

In Appendix B we describe two methods for numerical calculation of the phase shifts by solving an ordinary differential equation. The numerical calculation shows that $\Delta(k)$ for large k tends to a constant value $c=-\pi\phi^2$. An analytical proof for this result can be obtained using the WKB approximation (22) for the phase shift. In Fig. 1 we have plotted the function $\Delta(k)-c$ for $\phi=4.5$ and $d=1$. The numerical computation was performed for the magnetic fields B_1 and B_2 of Eqs. (2) and (3), respectively. In order to achieve convergence of Eq. (20) for $\phi=4.5$ we summed up to $l_{max}=20$ for the magnetic field B_2 and to $l_{max}=30$ for the Gaussian magnetic field B_1.

Figure 1 shows that the function $\Delta(k)-c$ tends rapidly to zero, apparently as $1/k^4$ for the magnetic field B_2 and faster for the magnetic field B_1, so the integral (19) is highly convergent. This is remarkable because it means that the same function $\Delta(k)$ can be used for the $(3+1)$-dimensional case, as can be seen from Eq. (26).

The result that the function $\Delta(k)-c$ corresponding to the magnetic field B_1 tends faster to zero than that for the magnetic field B_2 suggests that in general the function $\Delta(k)-c$ spreads when the corresponding magnetic field becomes more localized. This has been checked by calculations for magnetic fields other than B_1 and B_2 (see Sec. I). In addition we observed that when the magnetic field becomes more localized we need fewer values of l in order to achieve convergence of Eq. (20).

The value of the function $\Delta(k)$ at $k=0$ is independent of the magnetic field configuration and depends only on ϕ. This becomes evident if we take into account the Levinson theorem which is presented in Appendix A. Thus the two curves in Fig. 1 intersect at $k=0$. Now from the relations (19) and (20) we obtain

$$E_{eff(2+1)}=-\frac{1}{2\pi}\int_0^{+\infty}(\sqrt{k^2+m_f^2}-m_f)\frac{d[\Delta(k)-c]}{dk}dk. \tag{23}$$

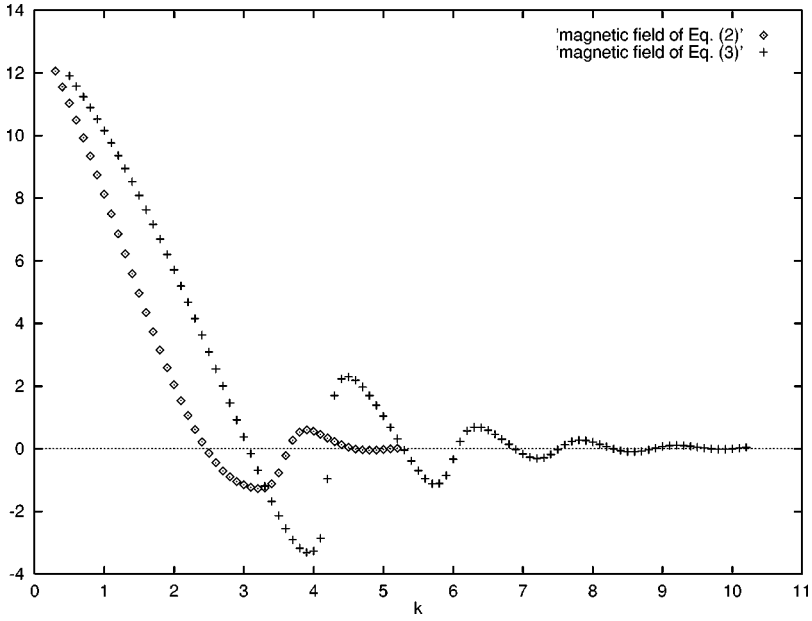

FIG. 1. $\Delta(k)-c$ as a function of k for $\phi=4.5$ and $d=1$.

Integrating by parts we find

$$E_{eff(2+1)}=\frac{1}{2\pi}\int_0^{+\infty}\frac{k}{\sqrt{k^2+m_f^2}}[\Delta(k)-c]dk. \qquad (24)$$

For the $(3+1)$-dimensional case, from the relations (14), (18), and (20), again dropping the free part from the density of states, we find

$$E_{eff(3+1)}=\frac{1}{4\pi^2}\int_0^{+\infty}(k^2+m_f^2)\ln\left(\frac{k^2+m_f^2}{m_f^2}\right)\frac{d[\Delta(k)-c]}{dk}dk$$
$$-\frac{1}{4\pi^2}\int_0^{+\infty}k^2\frac{d[\Delta(k)-c]}{dk}dk. \qquad (25)$$

Integrating by parts we obtain

$$E_{eff(3+1)}=-\frac{1}{2\pi^2}\int_0^{+\infty}k\ln\left(\frac{k^2+m_f^2}{m_f^2}\right)[\Delta(k)-c]dk. \qquad (26)$$

IV. DEPENDENCE ON THE RANGE d FOR FIXED MAGNETIC FLUX ϕ

A dimensional analysis shows that $\Delta(k)$ is a function of the form $F(kd,\phi)$. If we make the change of variable $y=kd$ and set $\Delta(k)=F(kd,\phi)$, we find

$$E_{eff(2+1)}=\frac{1}{2\pi d}\int_0^{+\infty}\frac{y}{\sqrt{y^2+m_f^2d^2}}[F(y,\phi)-c]dy, \qquad (27)$$

$$E_{eff(3+1)}=-\frac{1}{2\pi^2d^2}\int_0^{+\infty}y\ln\left(\frac{y^2+m_f^2d^2}{m_f^2d^2}\right)$$
$$\times[F(y,\phi)-c]dy, \qquad (28)$$

where d is a typical range of the magnetic field [see Eqs. (2) and (3)].

In Fig. 2 we see that $E_{eff(2+1)}$, for the Gaussian magnetic field B_1, is a positive decreasing function of d for fixed ϕ. The asymptotic behavior of $E_{eff(2+1)}$ for small values of d is proportional to $1/d$. This can be seen from relation (27). For large values of d we are in the weak field regime and $E_{eff(2+1)}$ is given approximately from the vacuum polarization diagram

$$E^{(2)}_{eff(2+1)}=\frac{1}{8\pi^2d}\int_0^1 dxx(1-x)$$
$$\times\int_0^{+\infty}dy\frac{y|\tilde{B}(y/d)|^2}{\sqrt{(m_fd)^2+x(1-x)y^2}}, \qquad (29)$$

where we have made the change of variable $q=y/d$ and $\tilde{B}(q)$ is the Fourier transform of the magnetic field. From the relation (29) we find that $E_{eff(2+1)}$ is proportional to $1/d^2$ for large values of d.

The curves in Fig. 2 appear to approach each other as d tends to infinity. Thus the effective energy for large d is proportional to ϕ^2. This is expected because the effective energy for large d is given approximately by the vacuum polarization diagram, which is proportional to ϕ^2.

In Fig. 3 we present our numerical results for the magnetic field B_2. We see that the effective energy as a function of d for fixed ϕ has the same features as those of the Gaussian magnetic field of Eq. (2).[5] Also we can see that the effective energy of B_2 is always bigger than the effective energy of B_1 for the same ϕ and d (this is also true for the

[5]We have checked that this is also true for the $(3+1)$-dimensional case. So the effective energy, in $3+1$ dimensions, is a negative increasing function of d for fixed magnetic flux (as shown in Fig. 4) for all magnetic fields of the form of the magnetic field of Eq. (1).

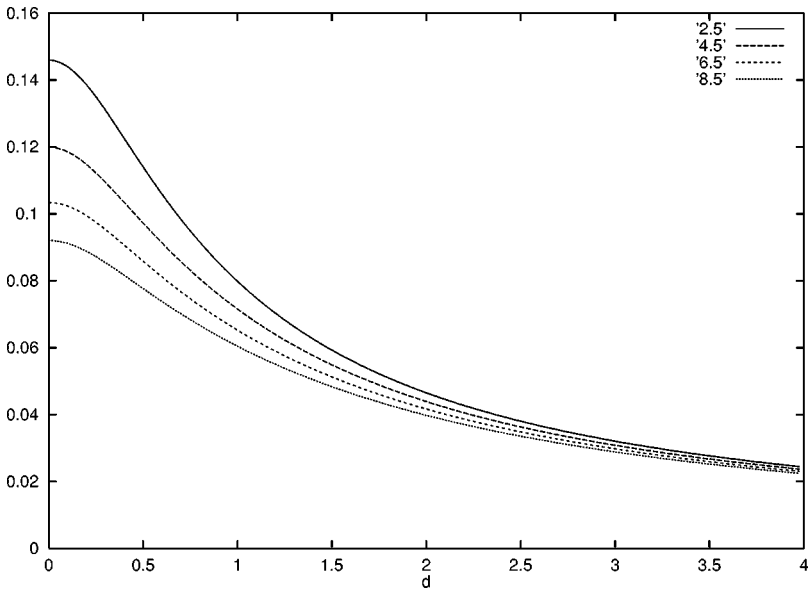

FIG. 2. $\phi^{-2}dE_{eff(2+1)}$ as a function of d for $\phi=2.5,4.5,6.5,8.5$ and $m_f=1$ for the Gaussian magnetic field of Eq. (2).

corresponding classical energies). This fact seems to be a consequence of the flux of the magnetic field B_2 being more concentrated than the flux of B_1.

The $(3+1)$-dimensional case, for the case of B_2, has already been studied with a different method by Bordag and Kirsten in Ref. [8]. Our results are shown in Fig. 4. They agree closely with those of Fig. 3 of Ref. [8].

The $(3+1)$-dimensional effective energy, for large d, is given by

$$E^{(2)}_{eff(3+1)}=-\frac{1}{8\pi^3 d^2}\int_0^1 dx x(1-x) \times\int_0^{+\infty} dy y|\tilde{B}(y/d)|^2\ln\left(\frac{m_f^2d^2+y^2x(1-x)}{m_f^2d^2}\right). \quad (30)$$

For $d\to+\infty$ we find

$$E^{(2)}_{eff(3+1)}=-\frac{1}{240\pi^3 m_f^2 d^4}\int_0^{+\infty} dy y^3|\tilde{B}(y/d)|^2. \quad (31)$$

For further discussion we will need the Fourier transforms of the magnetic fields of Eqs. (2) and (3):

$$\tilde{B}_1(q)=2\pi\phi\exp\left(-\frac{q^2d^2}{4}\right), \quad (32)$$

$$\tilde{B}_2(q)=4\pi\phi\frac{J_1(qd)}{qd}. \quad (33)$$

From the relation (31) we see that for large d the effective energy is proportional to $1/d^4$. This is true only for magnetic fields for which the integral (31) over y is convergent. An

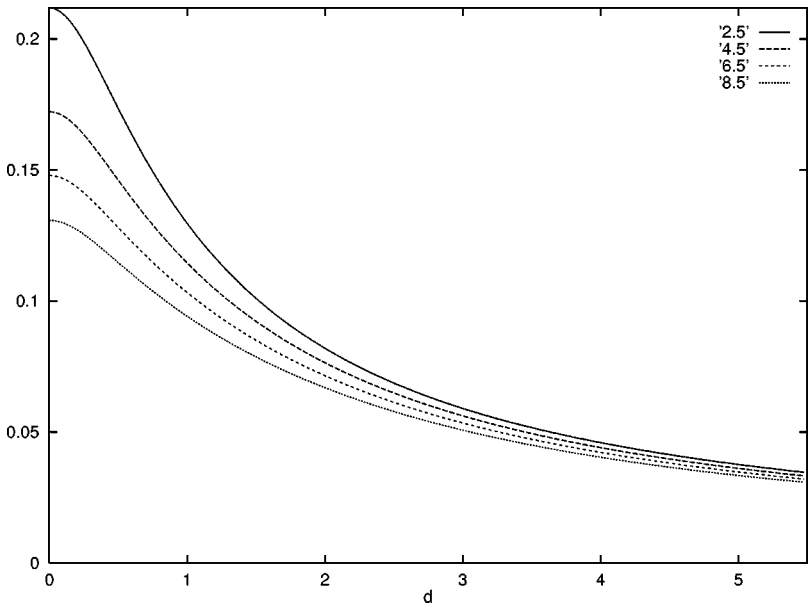

FIG. 3. $\phi^{-2}dE_{eff(2+1)}$ as a function of d for $\phi=2.5,4.5,6.5,8.5$ and $m_f=1$ for the magnetic field of Eq. (3).

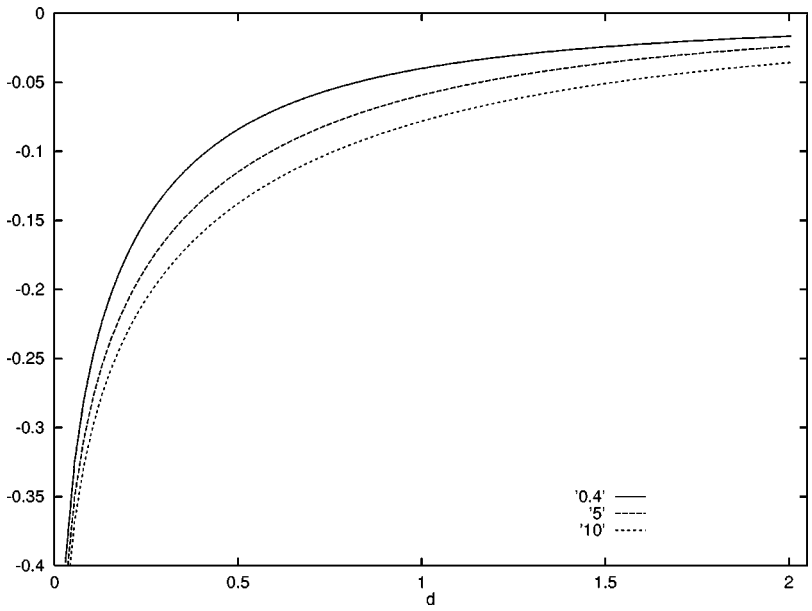

FIG. 4. $\phi^{-2}d^2E_{eff(3+1)}$ as a function of d for $\phi=0.4,5,10$ and $m_f=1$ for the magnetic field of Eq. (3).

example is the magnetic field B_1 with the Gaussian profile. For the magnetic field B_2 the integral (31) is divergent. We found numerically from Eq. (30) that in this case the asymptotic behavior is $O(1/d^{\alpha})$, where $3<\alpha<4$.

For small values of d, from the relations (28) and (13) we find the following asymptotic formula:

$$E_{eff(3+1)}=-\frac{1}{12\pi^2}\ln\left(\frac{1}{m_f d}\right)\int d^2\vec{x}B^2(\vec{x}). \tag{34}$$

The asymptotic formula (34) is the same as the one derived in Ref. [8]. From the relation (34) we obtain $E_{eff(3+1)}=(-\phi^2/3\pi d^2)\ln(1/m_f d)$ for the magnetic field B_2 and $E_{eff(3+1)}=(-\phi^2/6\pi d^2)\ln(1/m_f d)$ for the magnetic field B_1.

The total energy for B_2 is given by

$$E_{tot(3+1)}=E_{class(3+1)}+E_{eff(3+1)}$$

$$=\frac{2\pi\phi^2}{e^2d^2}+\frac{1}{d^2}f(m_f d,\phi) \tag{35}$$

where we have set $E_{eff(3+1)}=(1/d^2)f(m_f d,\phi)$. The physical meaning of the total energy is the energy we need to spend in order to create the magnetic flux tube. In this article we have computed this energy at one-loop order (i.e., we have not taken into account virtual photons). This approximation is valid only for small values of the coupling constant e.

For small values of d we find

$$E_{tot(3+1)}=\frac{2\pi\phi^2}{e^2d^2}-\frac{\phi^2}{3\pi d^2}\ln\left(\frac{1}{m_f d}\right). \tag{36}$$

We see that the logarithm, which comes from the effective energy part, dominates for small values of d. This asymptotic behavior of the total energy is not reliable. The reason is that small values of d correspond to magnetic fields whose Fourier transforms have contributions from high momenta at which the running coupling constant cannot be assumed small.

The asymptotic relation (36) for the total energy can be written in the form

$$E_{tot(3+1)}=\frac{2\pi\phi^2}{e_{eff}^2(d)d^2} \tag{37}$$

where we have defined a d-dependent effective coupling constant, for small values of d, according to

$$\frac{1}{e_{eff}^2(d)}=\frac{1}{e^2}-\frac{1}{6\pi^2}\ln\left(\frac{1}{m_f d}\right). \tag{38}$$

It is interesting to compare this to the B-dependent effective coupling constant of Ref. [15], for a homogeneous magnetic field, which for large B reads

$$\frac{1}{e_{eff}^2(B)}=\frac{1}{e^2}-\frac{1}{12\pi^2}\ln\left(\frac{B}{m_f^2}\right). \tag{39}$$

V. DEPENDENCE ON THE RANGE d FOR FIXED MAGNETIC FIELD STRENGTH $B_m=2\phi/d^2$

It is convenient to define a characteristic magnetic field strength as $B_m=\int\vec{B}\cdot d\vec{S}/\pi d^2$, in order to estimate the intensity of the magnetic field, where d is the range of the magnetic field. In the previous section we examined the dependence on d of the effective energy for fixed magnetic flux ϕ. Here, we study the dependence on d (or $m_f d$) for fixed magnetic field strength $B_m=2\phi/d^2$ (or B_m/m_f^2).

First, we examine the magnetic field of Eq. (3) [the Gaussian magnetic field of Eq. (2) is examined in the next section]. An interesting feature of this field [of Eq. (3)] is that when its range d increases it tends to a homogeneous magnetic field. Thus, in the homogeneous limit ($d\gg 1/\sqrt{B_m}$), we

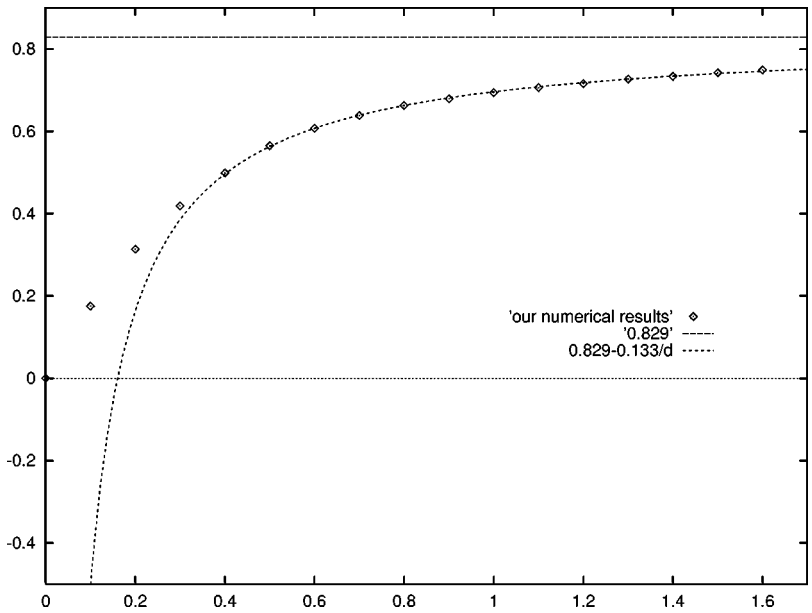

FIG. 5. $E_{eff(2+1)}/d^2$ as a function of d for $B_m=5$ and $m_f=1$ for the magnetic field of Eq. (3). The discrete points correspond to our numerical results and the continuous line to the best fit curve of the form a_0-a_1/d. The asymptotic value $a_0=0.829\pm0.002$ agrees quite well with that calculated from the Schwinger formula: 0.829. Our numerical results for a_0 and a_1 are rounded to three decimal points.

expect our numerical results to approach the result calculated from the Schwinger formula, which for the cases of $2+1$ and $3+1$ dimensions reads

$$E^{Sch}_{eff(2+1)}=\mathcal{A}\frac{B^{3/2}}{8\pi^{3/2}}\int_0^{+\infty}\frac{ds}{s^{3/2}}\left(\coth(s)-\frac{1}{s}\right)e^{-sm_f^2/B}, \tag{40}$$

$$E^{Sch}_{eff(3+1)}=\mathcal{A}\frac{B^{2}}{8\pi^{2}}\int_0^{+\infty}\frac{ds}{s^{2}}\left(\coth(s)-\frac{1}{s}-\frac{s}{3}\right)e^{-sm_f^2/B}, \tag{41}$$

where $\mathcal{A}$ is the area of the space box on the x-y plane and B is the magnetic field strength of the homogeneous magnetic field.

In Fig. 5 we have plotted the effective energy divided by d^2 for $B_m=5$ and $m_f=1$ for the magnetic field of Eq. (3). We see that $E_{eff(2+1)}/d^2$ is a positive increasing function of d which tends *very slowly* to an asymptotic value. The determination of this asymptotic value is not possible with a directly numerical computation, as for large values of d the numerical error of our method becomes significant. However, we see in Fig. 5 that our numerical results (for $d\geqslant0.4$) lie on a curve of the form a_0-a_1/d. Fitting a curve of this form to our data we obtain $a_0=0.829\pm0.002$ and $a_1=0.133\pm0.001$. The asymptotic value $a_0=0.829\pm0.002$ agrees quite well with that calculated from the Schwinger formula: $E^{Sch}_{eff(2+1)}/d^2=0.829$. This asymptotic behavior has also been observed for other values of B_m and m_f covering the whole range of the characteristic ratio B_m/m_f^2 that determines how strong is the magnetic field.

For small values of d, if we take into account the vacuum polarization diagram of Eq. (29) which is a good approximation for the effective energy, we find that $E_{eff(2+1)}/d^2$ is proportional to d. This is in agreement with the linear behavior of $E_{eff(2+1)}/d^2$ for $d\to0$, which is seen in Figs. 5 and 7 below.

In the case of $3+1$ dimensions, we see in Fig. 6 that our numerical results are negative and tend slowly to an asymptotic value, which also agrees closely with that calculated from the Schwinger formula of Eq. (41). The asymptotic behavior for large d is the same as that observed in the case of $2+1$ dimensions (a_0-a_1/d).

For small d we obtain from the vacuum polarization diagram of Eq. (30) that $E_{eff(2+1)}/d^2$ is proportional to $\ln d$. We see that this logarithmic behavior is not clear in Fig. 7 since we have not plotted enough points for small values of d. We avoided this, as in the region of small d $(d\approx0.1)$ the numerical accuracy we could achieve was not satisfactory.

A different way of finding the behavior of the effective energy for small d is to replace $F(y,\phi)=\phi F^{(1)}(y)+\phi^2F^{(2)}(y)$ in Eqs. (27) and (28) and take into account that the linear term is identically zero $(F^{(1)}(y)=0)$. We can prove that $F^{(1)}(y)=0$ using the first Born approximation for the phase shifts.

Our numerical work shows that there is a significant possibility that the $1/d$ term in the above-mentioned asymptotic behavior (a_0-a_1/d) is accurate. If, indeed, this behavior occurs, it would be interesting if one could give an analytical proof.

Note that this asymptotic behavior is expected only for discontinuous magnetic fields like the one of Eq. (3). In Fig. 7 we see that in the case of the Gaussian magnetic field of Eq. (2), our results for large d have the same asymptotic behavior as that of the derivative expansion b_0-b_1/d^2. This means that there is a remarkable difference between smooth and discontinuous magnetic fields, in the way their effective energies (divided by d^2) tend to their asymptotic values. It is obvious that this difference is related to the fact that the derivative expansion fails for discontinuous magnetic fields, like the magnetic field of Eq. (3).

VI. DERIVATIVE EXPANSION

An approximate way to compute the effective action in the presence of a static magnetic field is the derivative ex-

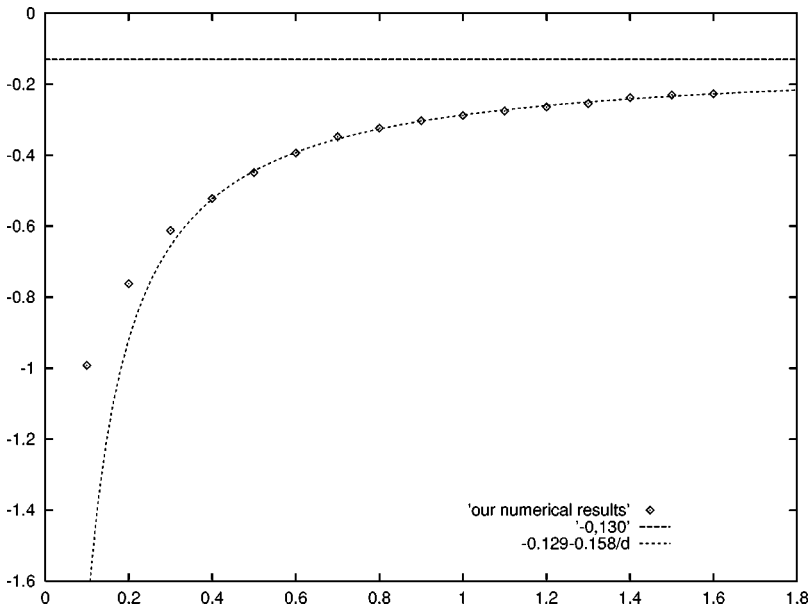

FIG. 6. $E_{eff(3+1)}/d^2$ as a function of d for $B_m=5$ and $m_f=1$ for the magnetic field of Eq. (3). The discrete points correspond to our numerical results and the continuous line to the best fit curve of the form a_0-a_1/d. The asymptotic value $a_0=0.129\pm0.002$ agrees quite well with that calculated from the Schwinger formula: 0.130. Our numerical results for a_0 and a_1 are rounded to three decimal points.

pansion. This method should give accurate results for slowly varying magnetic fields. Our aim is to examine cases in which the derivative expansion fails to provide a good approximation. Also, we can test our numerical results by comparing then with those of the derivative expansion in the homogeneous limit ($B_m d^2 \gg 1$), where the derivative expansion is expected to give accurate results.

The derivative expansion for $(3+1)$- and $(2+1)$-dimensional QED has been investigated in Refs. [17,16], respectively. For the case of $2+1$ dimensions, if we keep the first two terms (a zeroth order term plus a first order correction) the effective energy for a static magnetic field is given by

$$E^{der}_{eff(2+1)}=E^{(0)}_{(2+1)}+E^{(1)}_{(2+1)} \tag{42}$$

where

$$E^{(0)}_{(2+1)}=\int d^2\vec{x}\frac{B^{3/2}}{8\pi^{3/2}}\int_0^{+\infty}\frac{1}{s^{3/2}}\left(\coth(s)-\frac{1}{s}\right)e^{-sm_f^2/B}ds, \tag{43}$$

$$E^{(1)}_{(2+1)}=\frac{1}{8}\left(\frac{1}{4\pi}\right)^{3/2}\int d^2\vec{x}\frac{(\nabla B)^2}{B^{3/2}} \times\int_0^{+\infty}\frac{1}{s^{1/2}}e^{-sm_f^2/B}\left(\frac{d}{ds}\right)^3[s\coth(s)]ds. \tag{44}$$

For the special case of static magnetic fields, the above formulas were obtained in Refs. [18,19].

In Fig. 7 we have plotted the effective energy $E_{eff(2+1)}/d^2$ as a function of d, for fixed magnetic field strength $B_m=5$ and $m_f=1$ for the Gaussian magnetic field

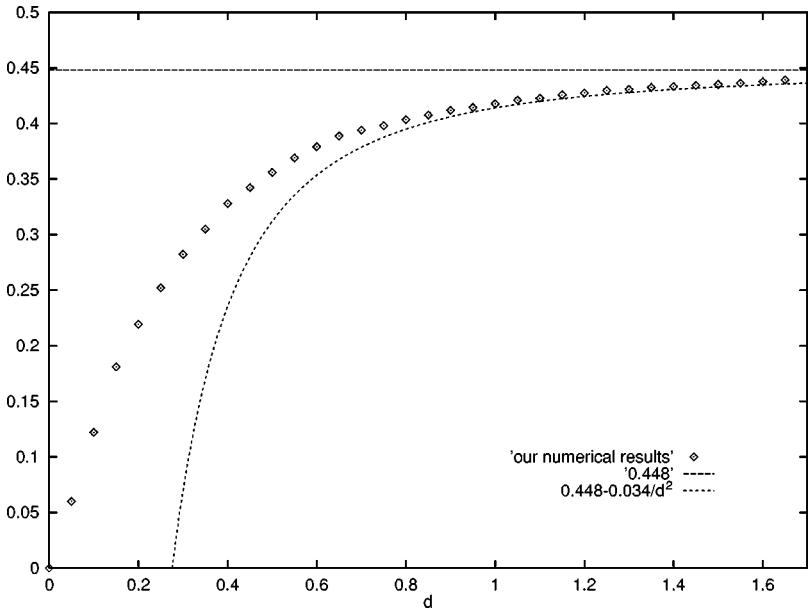

FIG. 7. $E_{eff(2+1)}/d^2$ as a function of d for $B_m=5$ and $m_f=1$ for the Gaussian magnetic field of Eq. (2). The discrete points correspond to our numerical results and the continuous line $0.448-0.034/d^2$ to the derivative expansion.

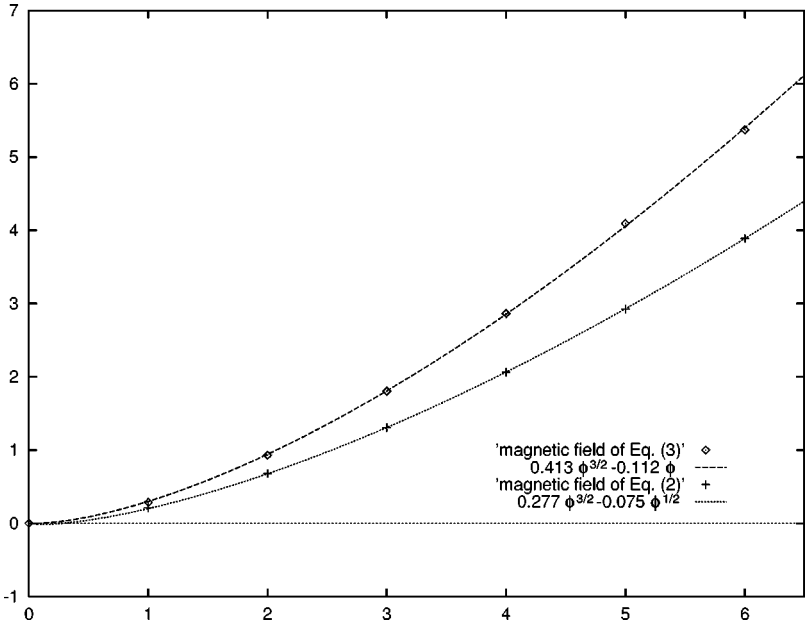

FIG. 8. $E_{eff(2+1)}$ as a function of ϕ for $d=1$ and $m_f=0$ for the magnetic fields of Eqs. (2) and (3). The discrete points correspond to our numerical results and the continuous lines to the best fit curves of the form $w_0\phi^{3/2}-w_1\phi$ for the magnetic field of Eq. (3) and $v_0\phi^{3/2}-v_1\phi^{1/2}$ for the magnetic field of Eq. (2). Our numerical results for the coefficients are rounded to three decimal points.

B_1. We see, as expected, that in the homogeneous limit ($d \gg 1/\sqrt{B_m}$) our results agree quite well with those of the derivative expansion. In the small d limit ($d \ll 1/\sqrt{B_m}$), the derivative expansion fails to approximate the effective energy. See the deviations in Fig. 7 for $d<0.8$.

The case of $3+1$ dimensions has not been included, as it is similar to the case of $2+1$ dimensions.

VII. THE STRONG MAGNETIC FIELD ($B_m \gg m_f^2$)

In order to study the strong magnetic field ($B_m \gg m_f^2$) behavior of the effective energy, we set $\Delta(k)=G(kB_m^{-1/2}, B_m d^2)$ and make the change of variable $y=kB_m^{-1/2}$ in relations (26) and (24):

$$E_{eff(2+1)}=\frac{B_m^{1/2}}{2\pi}\int_0^{+\infty}\frac{y}{\sqrt{y^2+m_f^2/B_m}}[G(y,B_m d^2)-c]dy, \tag{45}$$

$$E_{eff(3+1)}=-\frac{B_m}{2\pi^2}\int_0^{+\infty} y\ln\left(\frac{y^2+m_f^2/B_m}{m_f^2/B_m}\right) \times[G(y,B_m d^2)-c]dy, \tag{46}$$

where B_m is a characteristic magnetic field strength defined as $B_m=\Phi/\pi d^2$ and Φ is the magnetic flux.

For $B_m \gg m_f^2$ we find the asymptotic expressions

$$E_{eff(2+1)}=\frac{B_m^{1/2}}{2\pi}\int_0^{+\infty}[G(y,B_m d^2)-c]dy, \tag{47}$$

$$E_{eff(3+1)}=-\frac{B_m}{2\pi^2}\ln(B_m/m_f^2) \times\int_0^{+\infty} y[G(y,B_m d^2)-c]dy. \tag{48}$$

In the case of $3+1$ dimensions, if we take into account Eq. (13), we obtain an asymptotic formula for the case of strong magnetic field:

$$E_{eff(3+1)}=-\frac{1}{24\pi^2}\ln(B_m/m_f^2)\int_0^{+\infty} d^2\vec{x}B^2(\vec{x}). \tag{49}$$

The above equation is more general than Eq. (34), which was obtained in the limit $m_f d\to 0$ for fixed ϕ.

For fixed $m_f d$, Eq. (49) yields an asymptotic formula in the case of large magnetic flux ϕ:

$$E_{eff(3+1)}=-\frac{1}{24\pi^2}\ln(2\phi)\int_0^{+\infty} d^2\vec{x}B^2(\vec{x}). \tag{50}$$

From Eq. (50) we obtain $E_{eff(3+1)}=-(1/6\pi d^2)\phi^2\ln(2\phi)$ for the magnetic field of Eq. (3) and $E_{eff(3+1)}=-(1/12\pi d^2)\phi^2\ln(2\phi)$ for the magnetic field of Eq. (2). We see that for large ϕ the $(3+1)$-dimensional effective energy is proportional to $-\phi^2\ln\phi$. Also, this analytical result explains the weak dependence on ϕ of $E_{eff(3+1)}/\phi^2$ for the magnetic field of Eq. (3), which was observed numerically in Ref. [8].

In the case of $2+1$ dimensions, the asymptotic formula for $\phi\to+\infty$ is obtained from Eq. (45) by setting $m_f=0$. In Fig. 8 we have plotted the effective energy as a function of ϕ for $d=1$ and $m_f=0$, for the magnetic fields of Eqs. (2) and (3). Also, in the same figure we see that the curves $w_0\phi^{3/2}-w_1\phi$ and $v_0\phi^{3/2}-v_1\phi^{1/2}$, which correspond to the magnetic fields of Eq. (2) and (3), fit our data very well. Thus, for large ϕ the $(2+1)$-dimensional effective energy is proportional to $\phi^{3/2}$. Also, we observe that the coefficients $w_0=0.413\pm0.008$ and $v_0=0.2769\pm0.0005$ agree closely with the coefficients obtained from the formula

$$E_{eff(2+1)} = -\frac{\zeta(-1/2)}{\sqrt{2}\pi}\int d^2\vec{x}\, B^{3/2}(\vec{x}), \tag{51}$$

which are 0.416 for the magnetic field of Eq. (3) and 0.2772 for the magnetic field of Eq. (2). This formula is obtained from the leading term of the derivative expansion [given by Eq. (43)] if we set $m_f=0$. Our numerical results show that formula (51) gives the asymptotic behavior for large ϕ, in the case of $2+1$ dimensions. Note that formula (51) does not include all the cases of strong magnetic field $B_m=2\phi/d^2$. In the case of small $m_f d$ and fixed ϕ it is not correct. In this case the effective energy is proportional to $1/d$ as shown by Eq. (27) in Sec. IV.

VIII. CONCLUSIONS

We presented a numerical study of the fermion-induced $3+1$ and $2+1$ QED effective actions in the presence of any static cylindrically symmetric magnetic field with a finite magnetic flux. We used a simple novel approach for fast computation of the effective action. The numerical work was greatly facilitated by the observation that the function $\Delta(k)-c$ [see Eq. (20)] tends rapidly to zero for large k. The integrals (27) and (28) for the effective energy for $(2+1)$- and $(3+1)$-dimensional QED, respectively, are rendered convergent due to this fact.

The function $\Delta(k)-c$ is the only quantity we need to know in order to compute the effective energy [see Eqs. (27) and (28)]. We have performed computations for eight magnetic field configurations (see Sec. I). The form[6] of the function $\Delta(k)-c$ is similar for all these fields. This means that our conclusions for the effective energy are quite general and are not valid just for the magnetic fields of Eqs. (2) and (3).

For $e^2/4\pi=1/137$, our numerical work shows that for the families of magnetic fields we examined, there is no radius d of the magnetic flux tube that minimizes the total energy for fixed magnetic flux. The main reason for this is the small contribution (of the order of 1%) of the effective energy to the total energy. An exception, where the contribution is not small, is the case of $(3+1)$-dimensional effective energy for small d, as may be seen from Eq. (36).

In Sec. V, we observed that our numerical results for E_{eff}/d^2, in the case of the magnetic field of Eq. (3), converge slowly to an asymptotic value given by the Schwinger formula for a homogeneous magnetic field. In addition, we showed numerically that this asymptotic behavior for large d is of the form a_0-a_1/d. The case of the Gaussian magnetic field of Eq. (2) is different, as the convergence to the asymptotic value is considerably faster than the case of the magnetic field of Eq. (3). The asymptotic behavior of $E_{eff}/d^2 \sim b_0-b_1/d^2$ in this case, as we see in Fig. 7, is the same as that given by the derivative expansion. Generalizing, we expect that this behavior will be valid for all smooth magnetic fields of the form we examine. In the case of discontinuous magnetic fields, for which the derivative expansion fails, we expect a different asymptotic behavior of the form a_0-a_1/d.

We studied the case of large magnetic flux ϕ (strong magnetic field) when the spatial size of the magnetic flux tube is fixed. We showed that the effective energy for large ϕ is proportional to $-\phi^2\ln\phi$ in the case of $3+1$ dimensions and to $\phi^{3/2}$ in the case of $2+1$ dimensions. In particular, in the case of $3+1$ dimensions, we derived an explicit formula for large magnetic flux ($\phi \gg 1$).

It would be interesting if for large ϕ the effective energy in the presence of an inhomogeneous magnetic field became greater than the classical energy. In view of the above-mentioned results we can exclude this possibility at least for the class of inhomomogeneous magnetic fields of the form of a flux tube. An exception may be the case of $3+1$ dimensions for very large ϕ. However, for very large ϕ the asymptotic behavior $-\phi^2\ln\phi$ is not reliable, as the contributions of the higher loop corrections (two-loop corrections, three-loop corrections, etc.) to the QED effective energy cannot be assumed small.

ACKNOWLEDGMENTS

I am grateful to Professor G. Tiktopoulos, who proposed this topic to me and supervised the work. I also would like to thank him for numerous valuable discussions and the careful reading of the manuscript, as well as Dr. J. Alexandre, and Professor K. Farakos, Professor G. Koutsoumbas, and Professor A. Kehagias for useful comments and suggestions. This work was partially supported by NTUA program Archimides.

APPENDIX A: EFFECTIVE ENERGY FOR MASSLESS FERMIONS

In this appendix we derive an expression for the effective energy for massless fermions, since Eq. (14) contains a singularity at $m_f=0$. It is remarkable that this singularity does not exist in the unrenormalized effective energy of Eq. (12). It arises due to the renormalization procedure used to remove the ultraviolet divergent part of the effective energy. However, the above-mentioned singularity does not appear if instead of the renormalization condition $\Pi(0)=0$ we use the off-shell renormalization condition $\Pi(-M^2)=0$.

Setting $m_f=0$ in the unrenormalized effective energy of Eq. (12) we find

$$E_{eff(3+1)} = \frac{L_z}{4\pi}\sum_{\{n\}} E_{\{n\}} \ln\left(\frac{E_{\{n\}}}{\Lambda^2}\right) - \frac{1}{4\pi}\sum_{\{n\}} E_{\{n\}}. \tag{A1}$$

The ultraviolet divergent part in the above equation is removed if we include the following counterterm in the QED Lagrangian:

$$S_{count} = (Z_3-1)\int d^4x\left(-\tfrac{1}{4}F_{\mu\nu}F^{\mu\nu}\right) \tag{A2}$$

where

[6] See Sec. III and Fig. 1.

$$Z_3 = 1 - \frac{1}{2\pi^2}\left[\frac{1}{6}\ln\left(\frac{\Lambda^2}{M^2}\right) + \frac{5}{18}\right]. \tag{A3}$$

This counterterm is defined uniquely by the off-shell renormalization condition $\Pi(-M^2)=0$. In this case the renormalized effective action for massless fermions is

$$E^{(ren)}_{eff(3+1)} = \frac{L_z}{4\pi}\sum_{\{n\}} E_{\{n\}} \ln\left(\frac{E_{\{n\}}}{\Lambda^2}\right) + \frac{L_z}{6\pi}\sum_{\{n\}} E_{\{n\}}. \tag{A4}$$

In a similar way to that of Sec. III, we obtain

$$E^{(ren)}_{eff(3+1)} = \frac{1}{d^2}[c_1(\phi)\ln(dM) + c_2(\phi)] \tag{A5}$$

where

$$c_1(\phi) = \frac{1}{\pi^2}\int_0^{+\infty} y[F(y,\phi) - c]dy = \frac{d^2}{12\pi^2}\int \vec{B}^2(\vec{x})d^2\vec{x}, \tag{A6}$$

$$c_2(\phi) = -\frac{1}{\pi^2}\int_0^{+\infty} y\ln(y)[F(y,\phi) - c]dy - \frac{5}{6}c_1(\phi). \tag{A7}$$

The total energy is given by the equation

$$E_{tot} = E_{class} + E_{eff} = \frac{1}{2e_M^2}\int \vec{B}^2(\vec{x})d^2\vec{x} + \frac{1}{d^2}[c_1(\phi)\ln(dM) + c_2(\phi)] \tag{A8}$$

where e_M is the charge of the fermion defined at the scale M. The transformation law for the charge e_M is given by the equation

$$\frac{1}{e^2_{M'}} = \frac{1}{e^2_M} - \frac{1}{6\pi^2}\ln\left(\frac{M'}{M}\right) \tag{A9}$$

which also guarantees that the total energy is independent of the renormalization scale M.

APPENDIX B: THE APPEARANCE OF METASTABLE STATES FOR LARGE MAGNETIC FLUX ϕ

In this appendix we examine the appearance of metastable states for large magnetic flux ϕ. Note that in the large magnetic flux $\phi = B_m d^2/2$ limit we distinguish two cases: (a) a large magnetic field strength B_m keeping d constant and (b) a long range d of the magnetic field keeping B_m constant.

In Fig. 9, we see that the function $\delta_{l,s}(k)$ exhibits jumps at a finite number of values of k. Every jump increases the phase shift by π and corresponds to a metastable state of the electron. It is remarkable that these jumps occur in a small but nonzero interval Δk where the density of states appears as a very sharp peak. For the calculation of the phase shifts in this case we have used the differential equation (D14) of Appendix D, which is appropriate for large ϕ. For the plot we calculated the phase shifts with a step equal to 0.1. It may be noted, incidentally, that our numerical results for the phase shifts at $k=0$ are in agreement with Levinson's theorem [20]. Levinson's theorem, for a two-dimensional Schrödinger equation and for a potential with asymptotic behavior $O(1/r^2)$ for large r, has been investigated in Ref. [21]. Thus for our special case

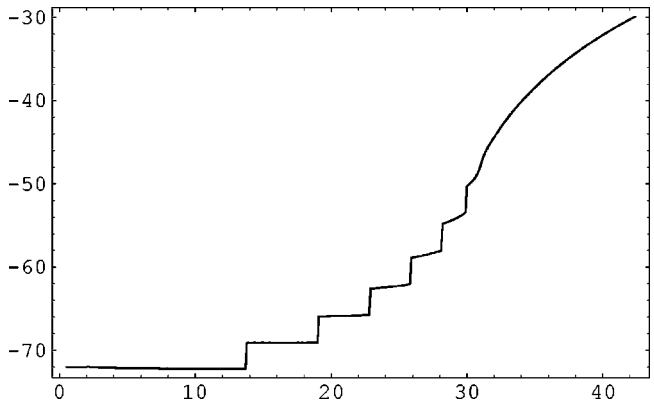

FIG. 9. $\delta_{l,\sigma}(k)$ as a function of k for $l=1$, $\sigma=1$, $d=1$, and $\phi=50$ for the Gaussian magnetic field of Eq. (2).

$$\delta_{l,s}(0) = \begin{cases} \pi + \dfrac{\pi}{2}(|l| - |l-\phi|) & \text{if a zero mode exists,} \\ \dfrac{\pi}{2}(|l| - |l-\phi|) & \text{otherwise.} \end{cases} \tag{B1}$$

The metastable states are due to the potential well form of the effective potential $v_{l,\sigma}(r) + (l^2 - 1/4)/r^2$ as shown in Fig. 10. It is interesting to compare our results with the WKB approximation for the eigenvalues k_n^2 of the metastable states as roots of the equation

$$\int_a^b \left(\sqrt{k_n^2 - v_{l,s}(r) - \frac{l^2}{r^2}}\right) dr = (n + \tfrac{1}{2})\pi, \quad n = 0,1,2,\ldots, \tag{B2}$$

where a and b are the turning points. In Table I we see that

TABLE I. We compare the energies of the metastable states as they are obtained from Fig. 9 with the WKB approximation results for $d=1$, $l=1$, $\sigma=1$, and $\phi=50$.

n	WKB approximation k_n	Numerical computation
1	13.721	13.7–13.8
2	19.051	19.0–19.1
3	22.881	22.8–22.9
4	25.854	25.8–25.9
5	28.200	28.1–28.2
6	29.997	29.9–30.0

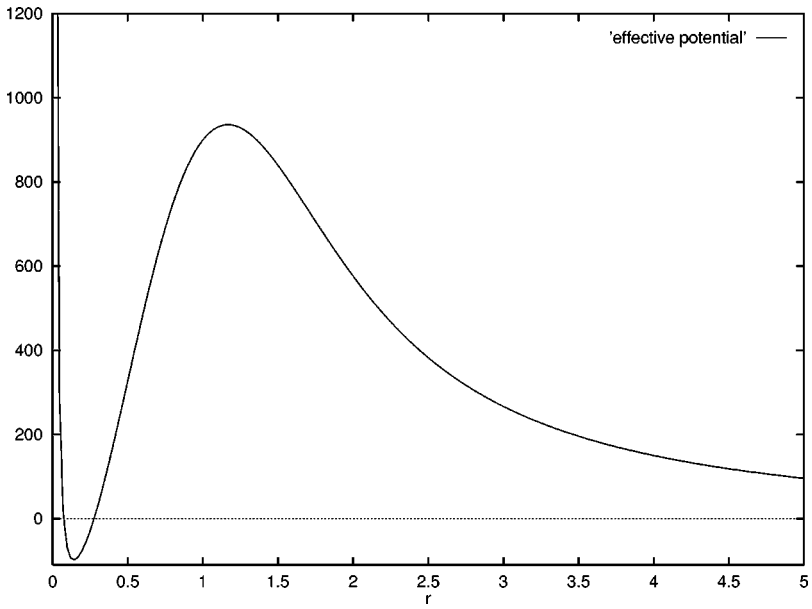

FIG. 10. $v_{l,\sigma}(r)+(l^2-1/4)/r^2$ as a function of r for $l=1$, $\sigma=1$, $d=1$, and $\phi=50$ for the Gaussian magnetic field of Eq. (2).

our numerical results agree closely with those of WKB approximation. Note that the electron metastable state energies corresponding to the eigenvalues k_n^2 are $\sqrt{k_n^2+m_f^2}$.

APPENDIX C: THE ROLE OF THE LANDAU LEVELS FOR THE EFFECTIVE ACTION

Taking into account Eqs. (9) and (14), it is obvious that the effective energy is determined uniquely by the spectrum of the eigenvalue equation $(\gamma^m D_m)^2 \Psi_{\{n\}}(x)=E_{\{n\}}\Psi_{\{n\}}(x)$. In Sec. V, it was shown numerically that the effective energy of a magnetic flux tube of the form of Eq. (3) tends (for $d \gg 1/\sqrt{B_m}$) to the result calculated from the Schwinger formula for a homogeneous magnetic field. One may think that this is unexpected, as the spectrum of a magnetic flux tube is continuous (with zero modes if $\phi>1$) whereas the spectrum of a homogeneous magnetic field, has a different structure—it is discrete and consists of the well known Landau levels. According to Appendix C these two spectra are related in the limit of large d. Indeed, if in the analysis of Appendix C, instead of the Gaussian magnetic field of Eq. (2), we used the magnetic field of Eq. (3) we would find metastable states with energies almost identical with those of the Landau levels (we have checked this numerically). Thus, the continuous spectrum of the magnetic field of Eq. (3) approaches, for $d \gg 1/\sqrt{B_m}$, the discrete spectrum of a homogeneous magnetic field in a straightforward way: each metastable energy level approaches a corresponding Landau level and at the same time more metastable states are added at the high energy end.

APPENDIX D: NUMERICAL CALCULATION OF THE PHASE SHIFTS

In this appendix we describe two methods for the numerical calculation of the phase shifts.

We will adapt the method presented by Farhy *et al.* in [22,23] to our problem. We consider two linearly independent solutions $u^{(1)}_{k,l,s}(r)$, $u^{(2)}_{k,l,s}(r)$ of the radial equation

$$\left(-\frac{d^2}{dr^2}+\frac{l^2-\frac{1}{4}}{r^2}+v_{l,s}(r)-k^2 \right) u_{k,l,s}(r)=0 \qquad \text{(D1)}$$

with asymptotic behavior $e^{\pm ikr}$ as r tends to infinity.

We can put these solutions into the form

$$u^{(1)}_{k,l,s}(r)=e^{i\beta_{l,s}(k,r)}\sqrt{r}H^{(1)}_l(kr), \qquad \text{(D2)}$$

$$u^{(2)}_{k,l,s}(r)=e^{i\beta^*_{l,s}(k,r)}\sqrt{r}H^{(2)}_l(kr), \qquad \text{(D3)}$$

where $H^{(1)}_l(x)$ and $H^{(2)}_l(x)$ are the Hankel functions of the first and second kind, respectively. The complex function $\beta_{l,s}(k,r)$ tends to zero as r tends to infinity.

The scattering solutions $u_{k,l,s}(r)$ of the radial equation (D1) satisfy the following boundary conditions:

$$u_{k,l,s}(0)=0, \qquad \text{(D4)}$$

$$u_{k,l,s}(r\to+\infty)\sim\cos\left(kr-\frac{\pi}{4}-\frac{l\pi}{2}+\delta_{l,s}(k) \right). \qquad \text{(D5)}$$

The solutions $u_{k,l,s}(r)$ are expressed as a linear combination of the solutions (D2) and (D3):

$$u_{k,l,s}(r)=e^{i\delta_{l,s}}e^{i\beta_{l,s}}\sqrt{r}H^{(1)}_l(kr)+e^{-i\delta_{l,s}}e^{-i\beta^*_{l,s}}\sqrt{r}H^{(2)}_l(kr). \qquad \text{(D6)}$$

Imposing the boundary condition (D4) on the solution (D6) we obtain

$$\delta_{l,s}(k)=-\mathrm{Re}\,\beta_{l,s}(k,0). \qquad \text{(D7)}$$

Substituting the solution (D2) into Eq. (D1) we obtain the differential equation

$$i\beta''_{l,s}(k,r)+2ik\,q_l(kr)\beta'_{l,s}(k,r)-[\beta'_{l,s}(k,r)]^2-v_{l,s}(r)=0 \tag{D8}$$

where

$$q_l(x)=\frac{d}{dx}\{\ln[\sqrt{x}H_l^{(1)}(x)]\}. \tag{D9}$$

The functions $\beta_{l,s}(k,r)$ should satisfy the following conditions:

$$\beta_{l,s}(k,+\infty)=0, \tag{D10}$$

$$\beta'_{l,s}(k,+\infty)=0. \tag{D11}$$

Because the potential tends to zero very slowly $O(1/r^2)$, we begin the numerical integration of the differential equation (D8) from a large number r_{max} toward zero, with the conditions

$$\beta_{l,s}(k,r_{max})=(-2l\phi+\phi^2)\frac{1}{2k\,r_{max}}, \tag{D12}$$

$$\beta'_{l,s}(k,r_{max})=-(-2l\phi+\phi^2)\frac{1}{2k\,r_{max}^2}. \tag{D13}$$

The above asymptotic behavior of the functions $\beta_{l,s}(k,r)$ can be obtained from Eq. (D8).

Another way to compute the phase shifts is by solving the differential equation

$$\frac{d\delta_{l,s}(k,r)}{dr}=-\frac{\pi}{2}r\,v_{l,s}(r)[J_l(kr)\cos\delta_{l,s}(k,r) - N_l(kr)\sin\delta_{l,s}(k,r)]^2 \tag{D14}$$

with the boundary condition $\delta_{l,s}(k,0)=0$, where $J_l(x)$ and $N_l(x)$ are the Bessel and Neumann functions, respectively. The phase shift is given by the limit

$$\delta_{l,s}(k)=\lim_{r\to+\infty}\delta_{l,s}(k,r). \tag{D15}$$

This method was formulated by Calogero in Ref. [24] for the three-dimensional case. It was obtained for two dimensions in Ref. [25].

For the numerical computations of the phase shifts we have used mainly the differential equation (D8) because it gives results faster and more accurately than Eq. (D14). However, this differential equation is stiff for large values of ϕ and small values of l. In that region of ϕ and l we have used Eq. (D14).

We also compared our numerical results with those of the WKB approximation (22) and we found good agreement for large l or large k.

[1] W. Heisenberg and H. Euler, Z. Phys. **38**, 314 (1936).
[2] V. Weisskopf, K. Dan. Vidensk. Selsk. Mat. Fys. Medd. **14**, 6 (1936).
[3] J. Schwinger, Phys. Rev. **82**, 664 (1951).
[4] A.N. Redlich, Phys. Rev. D **29**, 2366 (1984).
[5] D. Cangemi, E. D'Hoker, and G. Dunne, Phys. Rev. D **52**, 3163 (1995).
[6] G. Dunne and T. Hall, Phys. Lett. B **419**, 322 (1998).
[7] M.P. Fry, Phys. Rev. D **51**, 810 (1995).
[8] M. Bordag and K. Kirsten, Phys. Rev. D **60**, 105019 (1999).
[9] M. Scandurra, Phys. Rev. D **62**, 085024 (2000).
[10] G. Dunne, "Aspects of Chern-Simons theory," hep-th/9902115.
[11] J.O. Andersen and T. Haugset, Phys. Rev. D **51**, 3073 (1995).
[12] M. E. Peskin and D. V. Schroeder, *An Introduction to Quantum Field Theory* (Addison-Wesley, Reading, MA, 1995).
[13] Y. Aharonov and A. Casher, Phys. Rev. A **19**, 2461 (1979).
[14] B. Moussallam, Phys. Rev. D **40**, 3430 (1989).
[15] P. Elmfors, D. Person, and B.-S. Skagerstam, Phys. Rev. Lett. **71**, 480 (1993).
[16] D. Cangemi, E. D'Hoker, and G. Dunne, Phys. Rev. D **51**, 2513 (1995).
[17] H.W. Lee, P.Y. Pac, and H.K. Shin, Phys. Rev. D **40**, 4202 (1989).
[18] G. Dunne, Int. J. Mod. Phys. A **12**, 1143 (1997).
[19] V.P. Gusynin and I.A. Shovkovy, J. Math. Phys. **40**, 5406 (1999).
[20] L. Schiff, *Quantum Mechanics*, 3rd ed. (McGraw-Hill, New York, 1968).
[21] S.H. Dong, X.W. Hou, and Z.Q. Ma, "Levinson's Theorem for the Schrödinger Equation in Two Dimensions," quant-ph/9806004.
[22] E. Farhy, N. Graham, P. Haagensen, and R.L. Jaffe, Phys. Lett. B **427**, 334 (1998).
[23] N. Graham and R.L. Jaffe, Phys. Lett. B **435**, 145 (1998).
[24] F. Calogero, Nuovo Cimento **27**, 261 (1963).
[25] M.E. Portnoi and I. Galbrait, Solid State Commun. **103**, 325 (1997).